Inorganic Chemistry

ARTICLE

pubs.acs.org/IC

Metal-Free and Dicopper(II) Complexes of Schiff Base [2 + 2] Macrocycles Derived from 2,2′-Iminobisbenzaldehyde: Syntheses, Structures, and Electrochemistry

Scott A. Cameron and Sally Brooker*

Department of Chemistry and the MacDiarmid Institute for Advanced Materials and Nanotechnology, University of Otago, P.O. Box 56, Dunedin 9054, New Zealand

Supporting Information

ABSTRACT: Three new bis-terdentate Schiff base [2 + 2] macrocycles (H_2L^{Et}, H_2L^{Pr}, and H_2L^{Bu}) have been prepared in high yields by 1:1 condensation of 2,2′-iminobisbenzaldehyde with 1,2-diaminoethane, 1,3-diaminopropane, and 1,4-diaminobutane, respectively. Metalation of these macrocycles yields the corresponding dicopper(II) acetate (**1**, **2**, and **3**) and tetrafluoroborate (**4**, **5**, and **6**) complexes. The structures of H_2L^{Et}, H_2L^{Pr}, H_2L^{Bu}, $[Cu^{II}_2L^{i}(OAc)_2]\cdot$solvents (where i is Et, Pr or Bu) and $[Cu^{II}_2L^{Pr}(DMF)_4](BF_4)_2\cdot 0.5H_2O$ are reported. Intramolecular hydrogen bonding is a feature of the metal-free macrocycles. The copper(II) centers in $[Cu^{II}_2L^{i}(OAc)_2]\cdot$solvents are four coordinate, and the macrocycles have U-shaped (Et, Bu) or stepped (Pr) conformations. Complex **5** crystallizes with two dimethylformamide (DMF) molecules bound per five coordinate copper(II) center. Electrochemical studies revealed ligand based oxidations for all of the macrocycles and complexes. Complexes **1** and **2** undergo two quasi-reversible oxidations in DCM which are associated with the deposition of a visible film on the electrode after multiple scans in this oxidative region, suggestive of electropolymerization. Complexes **4**−**6**, studied in MeCN, have $Cu^{II} \rightarrow Cu^{I}$ redox potentials at more positive potentials than for **1**−**3**.

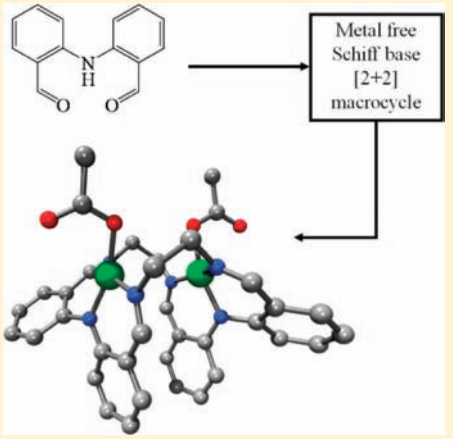

INTRODUCTION

There has been sustained interest in tetraimine [2 + 2] macrocycles since the first report of such a system, the Robson macrocycle,[1] in 1970 as they provide controlled access to dimetallic and tetrametallic complexes.[2−13] Many of the studies have focused on dicopper complexes.[10,14−22] Typically the structural, electrochemical and magnetic properties of these complexes have been investigated; and more recently their application as (oxidation, hydrolysis or esterification) catalysts;[23−25] anion binders;[26] or antimicrobial agents, DNA binding, or cleavage agents[27−29] have also been considered. These compounds have also been produced in to model enzyme functional sites.[30,31] Indeed there are many dicopper containing proteins, with important roles in oxygen activation and transport, electron transfer, methane oxidation, and so on.[32,33]

Schiff base [2 + 2] macrocycles can be obtained by condensation of a suitable dicarbonyl containing species ("head unit") with a diamine ("lateral unit").[2−13] Head units derived from pyridine, phenol, thiophenol, pyridazine, furan, thiophene, pyrrole, dipyrrole, pyrazole, and triazole have been employed for such purposes, with the pyridine and phenol based head units easily the most heavily used. Surprisingly the 2,2′-iminobisbenzaldehyde head unit (Scheme 1), available since 1983,[34] has been used only once, in the synthesis of a family of [1 + 1] macrocyclic complexes.[34] We decided to focus our attention on new Schiff base macrocycles based on this head unit, and report here the first examples of *dinucleating [2 + 2]* N_6 macrocycles derived from this head unit, obtained by condensation with simple nonsubstituted α,ω-diaminoalkanes (H_2L^{Et}, H_2L^{Pr}, and H_2L^{Bu}, Scheme 1).

We demonstrate that the resulting, metal-free, 22-, 24-, and 26-membered macrocycles can be easily deprotonated at the amine groups, forming dianionic macrocycles with two terdentate binding pockets that each bind a copper(II) ion (Scheme 1). The synthesis and characterization of these dinuclear copper(II) complexes was targeted to investigate the viability and profitability of employing such systems. The results of this study are presented here.

RESULTS AND DISCUSSION

Synthesis and Structure of 2,2′-Iminobisbenzaldehyde and Precursors. 2,2′-Iminobisbenzaldehyde was prepared according to the literature,[34] in comparable yields. First, an Ullmann coupling of ethyl 2-bromobenzoate and ethyl 2-aminobenzoate, in the presence of potassium carbonate and

Received: January 10, 2011
Published: March 21, 2011

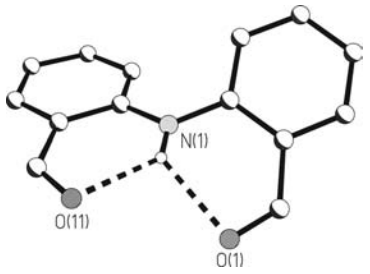

Figure 1. Perspective view of 2,2′-iminobisbenzaldehyde. Hydrogen atoms (except H1x) have been omitted for clarity. N(1)···O(1) 2.7707(18) Å; N(1)···O(11) 2.7510(17) Å. O(1)···H(1X)···O(11) 99.7(8)°.

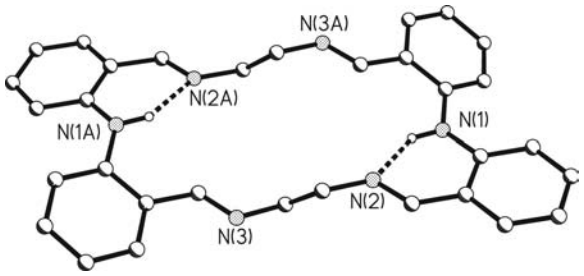

Figure 2. Perspective view of H_2L^{Et}. The second half of the molecule is generated by an inversion operation ($-x$, $1-y$, $-z$). Hydrogen atoms, other than those involved in hydrogen bonds, are omitted for clarity. N(1)···N(2) 2.7113(13) Å.

Scheme 1. Metal-Free Direct Synthesis of the Three [2 + 2] Schiff Base Macrocycles (n = 2, H_2L^{Et}; n = 3, H_2L^{Pr}; n = 4, H_2L^{Bu}) Derived from 2,2′-Iminobisbenzaldehyde, and Synthesis of Dicopper(II) Complexes of These Macrocycles As Acetate and Tetrafluoroborate Salts

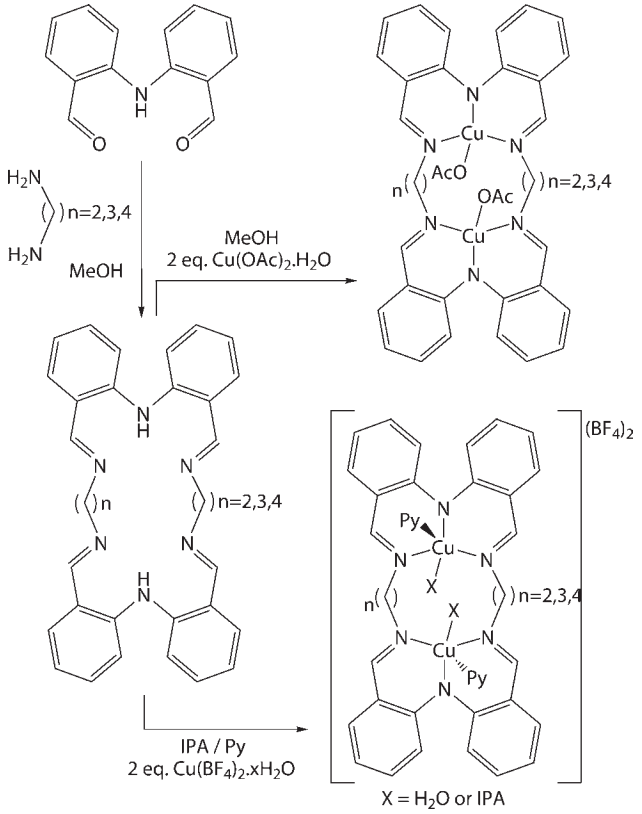

copper(I) iodide at 180 °C, is employed to form 2,2′-iminobis(ethyl benzoate), in 80% yield. This diester is reduced to the white diol, 2,2′-iminobis(hydroxymethylbenzene), using lithium aluminum hydride in dry diethyl ether, in 80% yield. Lastly, this diol is oxidized to the desired bright yellow dialdehyde using MnO_2 in dry diethyl ether in 72% yield.

Single crystals of these compounds were obtained as follows: light yellow blocks of the diester (Supporting Information, Figure S7) by recrystallization from pentane/DCM; yellow rods of the dialdehyde (Figure 1) by slow evaporation of Et_2O/MeOH.

To accommodate the hydrogen atoms present at the 6- and 6′-positions, the two phenyl rings of the diester and dialdehyde precursors are not coplanar; the resulting twist angle between the mean planes of these two phenyl rings is ∼43°. In both cases, the carbonyl groups are conjugated to the phenyl rings to which they are attached and do not deviate far from the mean planes of these rings. Strong intramolecular bifurcated hydrogen bonds (D···A ∼2.7 Å) are formed between the central amine hydrogen atom and both of the carbonyl oxygen atoms of these groups, and constrain the ester and formyl groups to be in a *cis*-like conformation relative to the amine.

Synthesis and Structure of Imine [2 + 2] Macrocyclic Ligands. The formation of [2 + 2] Schiff-base macrocycles is usually metal-templated, often on a metal ion other than that of interest thus necessitating a subsequent transmetalation reaction. However, in some cases they can be prepared directly, metal-free, usually by employing high dilution techniques or hydrogen bonding to favor cyclization.[35]

The target macrocycles, H_2L^{Et}, H_2L^{Pr}, and H_2L^{Bu} (Scheme 1), can be synthesized directly, in high yield and purity, by the Schiff-base condensation of 2 equiv of 2,2′-iminobisbenzaldehyde with 2 equiv of 1,2-diaminoethane, 1,3-diaminopropane, and 1,4-diaminobutane, respectively (in a similar fashion to the selenium and tellurium based macrocycles made by Singh and co-workers[36,37]). These new [2 + 2] macrocycles are particularly easily accessed as they precipitate from the refluxing methanol solution as they form. The resulting suspensions can be filtered after just 20 min, to give yellow powders that after drying under vacuum are analytically clean and air stable.

Light yellow single crystals (blocks) of H_2L^{Et}, H_2L^{Pr}, and H_2L^{Bu} were obtained by recrystallization from ethyl acetate. The ethylene and propylene linked macrocycles crystallized with half a molecule in the asymmetric unit whereas the butylene linked macrocycle crystallized with the entire molecule in the asymmetric unit (Figures 2−3 and Supporting Information, Figure S8). No solvent or disorder is present in these three structures.

In all cases there are strong intramolecular hydrogen bonds between the amine hydrogen atom and one or two imine nitrogen atoms (Supporting Information, Table S3). For the two macrocycles with an even number of methylene links (H_2L^{Et} and H_2L^{Bu}) there is one hydrogen bond per amine, and the imines are in a *trans*-like conformation. In contrast, the macrocycle with an odd number of methylene links (H_2L^{Pr}) forms two hydrogen bonds per amine (a bifurcated hydrogen bond), resulting in a *cis*-like conformation. The formation of the macrocycles is likely being promoted by these strong intramolecular hydrogen bonds.

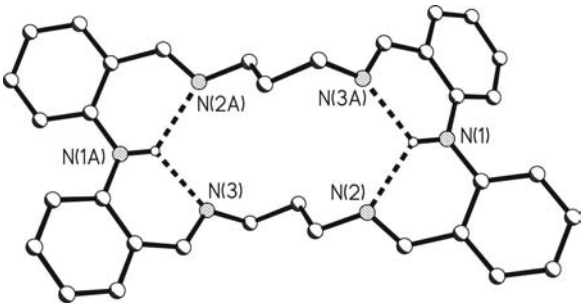

Figure 3. Perspective view of H_2L^{Pr}. The second half of the molecule is generated by an inversion operation ($-x$, $1-y$, $2-z$). Hydrogen atoms, other than those involved in hydrogen bonds, are omitted for clarity. N(1)···N(2) 2.7867(16) Å; N(1)···N(3A) 2.7922(16) Å. N(2)···H(1X)···N(3A) 107.5(8)°.

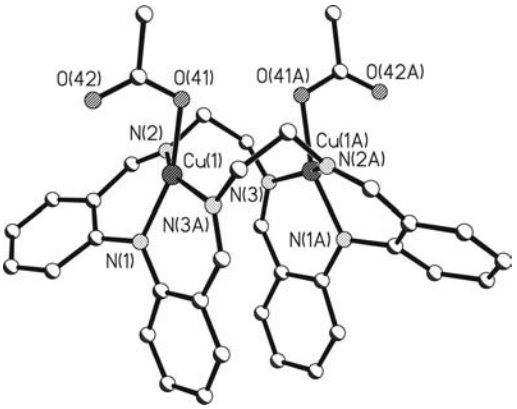

Figure 4. Perspective view of $[Cu^{II}_2L^{Et}(OAc)_2]$. The second half of the molecule is generated by a 2-fold rotation (y, x, $-z$). Hydrogen atoms are omitted for clarity.

The phenyl−phenyl twist angle for H_2L^{Et} is exceptionally low (28°), compared to any of the other ligands, ligand precursors or metal complexes (41−61°). In this structure the macrocycles sit on top of one another and there is a short edge-to-face π interaction from the C13−18 phenyl ring to the C1−6 ring of a neighboring unit. This particular interaction is not observed in any of the other structures and may be the cause of the low twist angle (for details of $\pi\cdots\pi$ interactions see Supporting Information, Tables S5 and S6; Figures S10−S18).

Synthesis and Structure of Macrocyclic Copper(II) Complexes. The dicopper(II) macrocyclic complexes were synthesized as acetate and tetrafluoroborate salts (Scheme 1). The acetate compounds (**1**, **2**, and **3**) could be simply produced by the addition of 2 equiv of copper(II) acetate monohydrate to a refluxing suspension of the appropriate macrocycle in dry MeOH. Upon addition the suspension immediately clarified and changed to a yellow-brown color. By ceasing heating and removing the condenser, dark orange-brown block-shaped single X-ray quality crystals of the ethylene, $[Cu^{II}_2L^{Et}(OAc)_2]$, propylene, $[Cu^{II}_2L^{Pr}(OAc)_2]\cdot 1.5MeOH\cdot 0.5H_2O$, and butylene $[Cu^{II}_2L^{Bu}(OAc)_2]\cdot 3MeOH$ linked macrocyclic dicopper(II) complexes were obtained in high yield.

The tetrafluoroborate complexes (**4**, **5**, and **6**) were produced in moderate yields by the addition of 2 equiv of copper(II) tetrafluoroborate hydrate to a hot suspension of the appropriate macrocycle in iso-propanol with a few drops of pyridine.

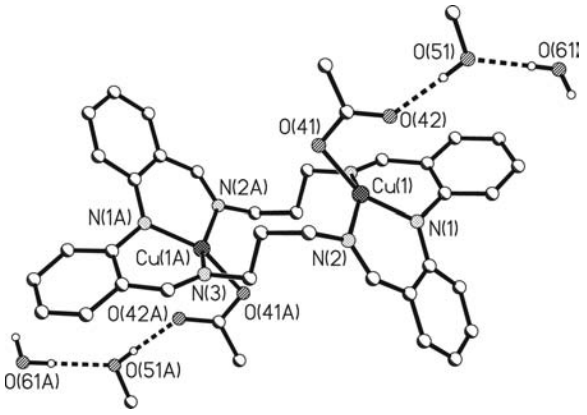

Figure 5. Perspective view of $[Cu^{II}_2L^{Pr}(OAc)_2]\cdot 1.5MeOH\cdot 0.5H_2O$. The second half of the molecule is generated by an inversion operation ($2-x$, $1-y$, $1-z$). Hydrogen atoms, other than those involved in hydrogen bonds, are omitted for clarity.

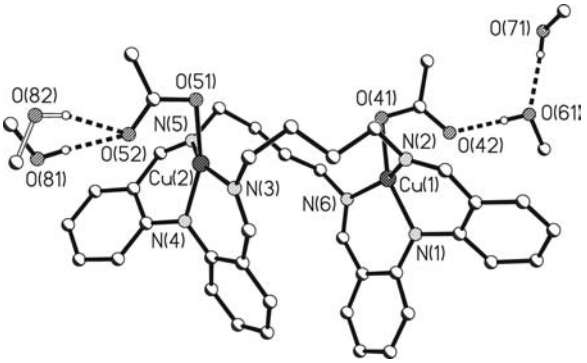

Figure 6. Perspective view of $[Cu^{II}_2L^{Bu}(OAc)_2]\cdot 3MeOH$. Hydrogen atoms, other than those involved in hydrogen bonds, are omitted for clarity.

Concentration of the resulting orange-brown solutions caused precipitation of the desired product, which was filtered and dried under vacuum. In all three cases, it appears that two solvent molecules are bound per copper(II) center, one pyridine and the other either water or iso-propanol, giving a square pyramidal coordination environment. Diethyl ether vapor diffusion into a dimethylformamide (DMF) solution of **5** yielded single crystals of $[Cu^{II}_2L^{Pr}(DMF)_4](BF_4)_2\cdot 0.5H_2O$.

The complexes $[Cu^{II}_2L^{Et}(OAc)_2]$, $[Cu^{II}_2L^{Pr}(OAc)_2]\cdot 1.5MeOH\cdot 0.5H_2O$ and $[Cu^{II}_2L^{Pr}(DMF)_4](BF_4)_2\cdot 0.5H_2O$ crystallized with half a macrocycle in the asymmetric unit whereas the entire macrocycle was present in $[Cu^{II}_2L^{Bu}(OAc)_2]\cdot 3MeOH$ (Figures 4−6 and Supporting Information, Figure S9). This is an analogous pattern to that in the free macrocycles; the reduced internal symmetry observed for the butylene linked macrocycle and complex may be attributable to the increased length, and hence flexibility, of the alkyl chain.

The bond lengths and angles involving the copper(II) centers in each of these complexes are provided in Supporting Information, Table S4. In all cases, the macrocyclic ligands are deprotonated at both of the amines (N1/N4), and these make the shortest Cu−N bond lengths. Despite the negative charge, the equatorially coordinated acetate oxygen atoms make the longest of the bonds to the copper centers. Nevertheless the Cu−X distances fall in a narrow range (1.922−1.995 Å). Likewise, all of

dx.doi.org/10.1021/ic200059n |*Inorg. Chem.* 2011, 50, 3697–3706

Table 1. Comparison of Selected Structural Parameters between the Ligand Precursors, Metal-Free Macrocycles, and the Corresponding Dicopper(II) Complexes, $[Cu^{II}_2(OAc)_2L^{Et}]$, $[Cu^{II}_2(OAc)_2L^{Pr}]\cdot 1.5MeOH\cdot 0.5H_2O$, $[Cu^{II}_2(OAc)_2L^{Bu}]\cdot 3MeOH$, and $[Cu^{II}_2L^{Pr}(DMF)_4]\cdot 0.5H_2O$

	crystal system (space group)	α(Ph-Ph) (deg)[a]	mean formyl/imine oop deviation and ranges (Å)[b]	hydrogen bonding D···A (Å)	copper ···copper separation (Å)	measure of metal geometry
BPhOEt	monoclinic ($P2_1/n$)	45.55(4)	0.366 0.266(2)−0.466(2)	N(1)···N(2) 2.7113(13)	N/A	N/A
BPhCHO	orthorhombic ($P2_12_12_1$)	41.08(4)	0.220 0.1743(3)−0.265(3)	N(1)···N(2) 2.7867(16) N(1)···N(3) 2.7922(16)	N/A	N/A
H_2L^{Et}	monoclinic ($P2_1/c$)	27.84(5)	0.323 0.259(2)−0.386(2)	N(1)···N(2) 2.7113(13)	N/A	N/A
H_2L^{Pr}	monoclinic ($P2_1/c$)	48.07(4)	0.169 0.161(2)−0.176(2)	N(1)···N(2) 2.7867(16) N(1)···N(3) 2.7922(16)	N/A	N/A
H_2L^{Bu}	triclinic ($P\bar{1}$)	50.20(11); 53.06(10)	0.159 0.105(5)−0.270(5)	N(1)···N(6) 2.670(3) N(3)···N(4) 2.683(3)	N/A	N/A
$[Cu^{II}_2(OAc)_2L^{Et}]$	trigonal ($P3_221$)	53.43(9)	0.288 0.127(6)−0.449(6)	nil	3.6072(8)	0.35 D_{4h}:T_d[c]
$[Cu^{II}_2(OAc)_2L^{Pr}]$ $\cdot 1.5MeOH\cdot 0.5H_2O$	triclinic ($P\bar{1}$)	54.91(12)	0.359 0.336−0.381(7)	O(41)···O(50) 2.724(5) O(50)···O(60) 2.896(19)	5.2650(17)	0.41 D_{4h}:T_d[c]
$[Cu^{II}_2(OAc)_2L^{Bu}]$ $\cdot 3MeOH$	monoclinic (Cc)	59.70(6); 55.25(5)	0.345 0.231(4)−0.461(4)	O(41)···O(60) 2.682(2) O(60)···O(70) 2.785(2) O(51)···O(80) 2.744(3) O(51)···O(81) 2.739(8)	5.8384(3)	0.38 D_{4h}:T_d[c] 0.31 D_{4h}:T_d[c]
$[Cu^{II}_2L^{Pr}(DMF)_4]$ $\cdot 0.5H_2O$	triclinic ($P\bar{1}$)	61.00(6)	0.272 0.065(3)−0.479(4)	O(51) ···O(61) 2.864(7) O(61) ···F(11) 2.607(7)	5.0207(5)	0.29 C_{4v}:D_{3h}[d]

[a] The angle between the mean planes of the two phenyl rings making up the diphenylamine unit. [b] The mean, and range, of out of plane (oop) deviation of the carbonyl oxygen and imine nitrogen atoms from the mean plane of the phenyl ring to which they are attached. [c] Tetrahedral distortion parameter [$\omega/90$]: Square Planar (D_{4h}), 0; Tetrahedral (T_d), 1, where ω is the dihedral angle between the chelate ring planes N−Cu−N and N−Cu−O.[38] [d] Trigonality distortion parameter $\tau = [(\beta-\alpha)/60]$: Square Pyramidal($C_{4v}$), 0; Trigonal Bipyramidal (D_{3h}), 1, where β is the largest of the basal angles and α is the second largest.[40]

the *cis* X−Cu−X angles (89.2−98.3°) are quite close to 90°. This is pleasing as these macrocycles were designed to form six-membered chelate rings on binding, and hence angles close to 90°. It is anticipated that this should prove favorable for most transition metal ions, so this is a very promising result with regard to our intention to further our investigations of such complexes.

In the acetate complexes the copper(II) ions are in a tetrahedrally distorted square planar N_3O environment (0.31−0.41 D_{4h}:T_d ratio,[38] see Table 1). This distortion is very noticeable when a mean plane produced from any three of the four donor atoms is considered, as in all cases the copper atom is somewhat out of plane (0.106−0.452 Å) while the fourth donor atom is even further out of plane (1.044−1.657 Å). The oxygen atom (from the acetate ion) is strongly bound in what is approximately the equatorial plane. This results in the second oxygen atom of the same acetate weakly interacting with the otherwise vacant "axial" site of the same copper center ($Cu-O_{ax}$ is ca. 0.5−0.9 Å > $Cu-O_{eq}$; Supporting Information, Table S4); however, as expected,[39] the resulting four-membered chelate ring has a rather acute O−Cu−O angle (50.2−58.6°).

In the tetrafluoroborate complex, the copper ions are five, not four coordinate, each binding *two neutral monodentate* solvent molecules (rather than one acetate anion). The result is a trigonally distorted square pyramidal N_3O_2 environment (0.29 C_{4v}:D_{3h} ratio (τ),[40] see Table 1). Two molecules of DMF bond to each copper center, one at the remaining equatorial site and one at the axial site. The latter DMF makes good angles to the 4 donors in the basal plane and shows the axial elongation expected for copper(II) ($Cu-O_{ax}$ being ~0.38 Å longer than the equatorial bond lengths, Supporting Information, Table S4).

The copper(II) centers are a significant distance apart (3.6−5.8 Å, Table 1), and are not bridged by any group. This distance increases with increasing chain length. Since the propylene linked

dx.doi.org/10.1021/ic200059n |*Inorg. Chem.* 2011, 50, 3697–3706

Table 2. Comparison of the Anodic and Cathodic Peak Potentials for Macrocycles H_2L^{Et}, H_2L^{Pr}, and H_2L^{Bu} and Complexes with Copper(II) Acetate (1, 2, and 3) and Tetrafluoroborate (4, 5, and 6), at 200 mV s^{-1} Scan Rate, Referenced against Internal Fc/Fc^+ Couple for Ease of Comparison[a]

E_{PA} and/or [E_{PC}], and where applicable {ΔE_P, the absolute difference between E_{PC} and E_{PA}}, in V versus Fc/Fc^+								
H_2L^{Et}	H_2L^{Pr}	H_2L^{Bu}	1	2	3	4	5	6
						0.468	0.512, 0.682	0.454, 0.534
0.025		−0.102	0.276 [0.130] {0.14}	0.332 [0.161] {0.17}	0.236	0.917	0.856	0.910
0.137	0.107	0.063	0.474 [0.297] {0.18}	0.506 [0.309] {0.20}	0.415	[−0.296]	[−0.933]	[−0.672]
		0.145	[−1.695] −0.793, −0.479	[−1.703] −0.471	[−1.94] −0.521	[−1.254]	[1.284] −0.500, −0.168	[−0.881] −0.520
						[−1.411]		[−1.611]

[a] The original data can be seen in Figures 7−9, in the discussion below, and in the Supporting Information. Note that for solubility reasons, complexes **4**−**6** were run in MeCN whereas all other samples were run in DCM.

macrocycle adopts a "stepped" conformation as opposed to the "U shaped" conformation for the ethylene and butylene complexes, the observed Cu···Cu separation, while falling between the values for the smaller and larger macrocycles, is slightly higher than might be expected. The tetrafluoroborate complex of the propylene linked macrocycle also exhibits the stepped conformation, and has a slightly shorter (0.24 Å) Cu···Cu separation than its acetate analogue.

As for the carbonyl groups in the precursors, the imine groups in the metal-free macrocycles and the resulting complexes do not deviate much from the mean plane of the phenyl ring to which they are attached (Table 1). As for the metal-free macrocycles, the phenyl rings are twisted away from coplanarity in all four structurally characterized copper(II) complexes (Figures 4−6 and Supporting Information, Figure S9, Table 1). Upon coordination to copper(II) the twist angle between these phenyl rings increases, by 5−26°, to a similar value for all complexes, $\alpha = 57 \pm 5°$. Notably, all precursors, ligands, and complexes have twist angles within a fairly small range ($50 \pm 10°$), except for the ethylene linked ligand, H_2L^{Et}, which has a significantly lower twist angle of 27.8° (discussed above). It therefore exhibits easily the largest increase in twist angle on complexation to copper(II), 26°, while the rest increase by only 5−13°. All of these compounds have significantly lower twist angles than those reported for the tellurium and selenium macrocycles of Singh and co-workers (63−83° free macrocycles; 67−87° when coordinated to Ni, Co, Pd).[36,37,41,42] This can be attributed to the amine nitrogen atom being somewhat more conjugated with the carbon atoms of the phenyl rings than is the case for the larger selenium and tellurium atoms.

The conformation of the macrocyclic complexes is interesting since the ethylene and butylene linked macrocyclic complexes form "U-shaped" structures, where the acetate anions are both on the same side of the macrocycle. In these structures, two of the four phenyl rings on opposite sides of the macrocycles are close to each other; the other two rings face outward. The ethylene linked structure crystallizes in a chiral space group ($P3_221$), whereby these phenyl rings are offset π-stacked and are always on the same side of the macrocycle. Presumably crystals of the opposite chirality also crystallized.

The butylene structure crystallizes in a non-centrosymmetric space group (Cc), which also features one pair of opposite phenyl rings close to each other, but forms a much weaker $\pi-\pi$ interaction. An *n*-glide generates the molecule of the opposite handedness. In contrast, the propylene linked macrocyclic complexes form "stepped" structures, where each acetate, or axial DMF points towards opposite sides of the macrocycles, and crystallize in centrosymmetric space groups. For details of the $\pi\cdots\pi$ interactions present in these complexes see the Supporting Information, Tables S5 and S6; Figures S15−S18.

There are multiple hydrogen bonds present in the structures of the copper(II) acetate complexes. These occur between the acetate groups and the solvent, and are quite strong (Table 1). Similarly, in the tetrafluoroborate complex, a water molecule hydrogen bonds to both an anion as well as the coordinated oxygen atom in the axially bound DMF molecule.

Electrochemical Studies. The cyclic voltammograms (CVs) of the macrocyclic ligands (H_2L^{Et}, H_2L^{Pr}, and H_2L^{Bu}) and copper(II) acetate (**1**, **2**, and **3**) and tetrafluoroborate (**4**, **5**, and **6**) complexes were investigated. For solubility reasons the ligands and acetate complexes were run in DCM versus Ag/AgCl (3 mol·L^{-1} KCl) (Fc/Fc^+ E_m 0.64 V; ΔE_p 0.17 V), whereas the tetrafluoroborate complexes were run in MeCN versus Ag/0.01 mol·L^{-1} $AgNO_3$ (Fc/Fc^+ E_m 0.10 V; ΔE_p 0.16 V). For ease of comparison the peak potentials for the observed oxidative and reductive processes, at a scan rate of 200 mV/s, have been converted to be referenced against internal Fc/Fc^+ and are presented in Table 2. However, in the following discussion and figures, it is important to note that all quoted potentials are versus the original reference electrode (not versus Fc/Fc^+). Various scan rate studies were also carried out for which the scan rates investigated were 25, 50, 100, 200, 300, and 400 mV/s (Supporting Information, Table S7).

Imine [2 + 2] Macrocyclic Ligands. The electrochemistry of the macrocycles H_2L^{Et}, H_2L^{Pr}, and H_2L^{Bu} was investigated in DCM versus Ag/AgCl (3 mol·L^{-1} KCl) (Figure 7) for comparison with the corresponding macrocyclic dicopper(II) complexes. In all three cases, irreversible oxidative processes occurred with E_{PA} values below 1 V (H_2L^{Et}, 0.66 and 0.77 V; H_2L^{Pr}, 0.74 V; H_2L^{Bu}, 0.53, 0.70, and 0.78 V). For H_2L^{Et}, there is one clear oxidation process and a lower current process at slightly lower potentials, which appears as a shoulder. Likewise for H_2L^{Bu}, there is one clear process, but it is flanked by both lower and higher potential processes of low current. In contrast, ligand H_2L^{Pr} has only one distinguishable oxidative process.

In all cases, on scanning to negative potentials first (0 → −1.7 → 0 V) there are no reductive processes, indicating that these ligands cannot be reduced at potentials more positive than −1.7 V (Supporting Information, Figures S24, S26 and S28). Scans to positive potentials first (0 → 1.3 → −1.7 → 0 V) reveal a very small reductive process having an E_{PC} at slightly more positive than −1 V (Figure 7), which is more obvious at higher scan rates (Supporting Information, Figures S23, S25 and S27).

dx.doi.org/10.1021/ic200059n |*Inorg. Chem.* 2011, 50, 3697–3706

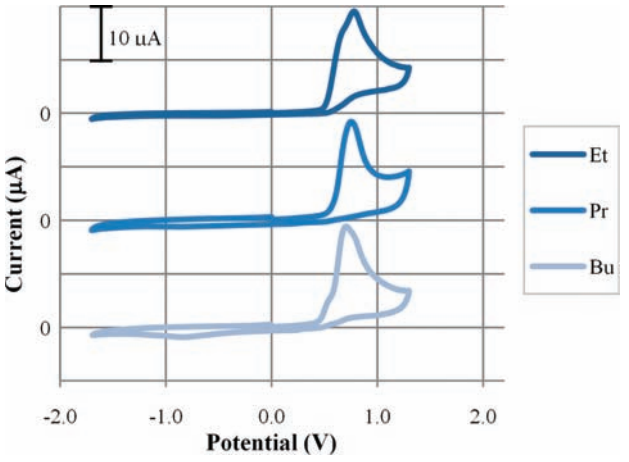

Figure 7. CVs (0 → 1.3 → −1.7 → 0 V) of macrocycles H_2L^{Et}, H_2L^{Pr}, and H_2L^{Bu} run at 200 mV/s in DCM versus Ag/AgCl (3 mol·L^{-1} KCl).

Copper(II) Acetate Macrocyclic Complexes. The electrochemistry of the copper(II) acetate complexes **1**, **2**, and **3** was investigated in DCM versus Ag/AgCl (3 mol·L^{-1} KCl) (Figure 8) since these compounds are only sparingly soluble in MeCN. The CVs of the ethylene linked dicopper(II) complex **1** show two clear oxidation processes with E_{PA} of about 0.91 and 1.11 V. These appear to be reversible as they have associated reduction processes with E_{PC} of about 0.76 and 0.93 V, and ΔE_P values of 0.15 and 0.18 V respectively, close to that observed for the Fc/Fc^+ couple in this cell system (ΔE_P = 0.17 V; not 57 mV due to IR drop which is particularly large in DCM). The ratio i_{PA}/i_{PC} is almost unity for both processes. In principle these processes could be due to copper oxidation ($Cu^{II} \rightarrow Cu^{III}$), but they are more likely to be due to ligand oxidation, given the results obtained on the free macrocycles (above). The shift of these oxidations to more positive potentials compared to the free macrocycle is expected because of the presence of the copper(II) cations which likely outweighs the effect of deprotonation.

Multiple scans of this oxidative region (0.3 → 1.5 → 0.3 V) were carried out to investigate the chemical reversibility of these oxidation processes (Supporting Information, Figure S35). Both the oxidation and return reduction waves showed sustained growth in peak current with each additional scan (without cleaning of the platinum working electrode). Inspection of the working electrode after 12 scans showed a bronze colored material had been thinly deposited on the surface (Supporting Information, Figure S39b). Further scans resulted in the two oxidative processes merging into one broad process. The same was observed for the two return reductive processes. After 100 scans the growth in peak current begins to slow, but it still continues to grow (Supporting Information, Figure S40). Furthermore, the color of the deposited material darkens (Supporting Information, Figure S39c). To ensure this electrodeposition was not a consequence of the Pt working electrode surface used, a glassy carbon (GC) electrode was also tried. The same behavior of increasing current with each scan was observed (Supporting Information, Figures S35 and S37) and a similar looking material was seen on the electrode surface afterward. In a final experiment to probe the nature of this behavior a small amount of MeCN was added to the DCM solution and the same tests with Pt and GC working electrodes were carried out. Under these conditions the processes grew only very, very slowly and kept their peak shape

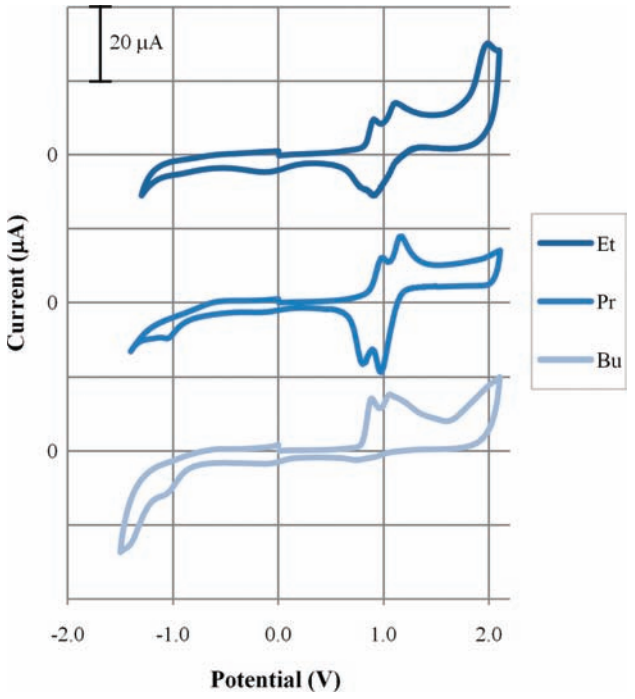

Figure 8. CVs (0 → 2.1 → about −1.4 → 0 V) of copper(II) acetate macrocyclic complexes **1**, **2**, and **3** run at 200 mV/s in DCM versus Ag/AgCl (3 mol·L^{-1} KCl).

(Supporting Information, Figures S36 and S38). It therefore seems that the product of this oxidative process is stabilized or solubilized by the MeCN, whereas use of only DCM causes deposition onto the electrode surface, modifying the electrode surface and resulting in higher current flows. This voltammetric behavior is consistent with ligand based oxidative polymerization and deposition.[43]

CVs of the propylene (**2**) and butylene (**3**) linked copper(II) acetate macrocyclic complexes in DCM also show two clear oxidation processes (**2**, E_{PA} 0.96 and 1.14 V; **3**, 0.87 and 1.04 V). A further oxidation process in **3** could be distinguished at 1.17 V at low scan rates (Supporting Information, Figure S48). As for **1**, return reduction processes having E_{PC} of 0.95 and 0.80 V were seen for **2**, giving ΔE_P values of 0.17 and 0.20 V, respectively, similar to that seen for Fc/Fc^+ in this system (0.17 V). These return waves had even better peak shapes, giving an i_{PA}/i_{PC} ratio of unity for both processes at all scan rates (Supporting Information, Figure S43). These two redox processes are thus also reversible. In contrast, **3** has no clear peaks on the return (even when the direction of the scan is reversed at 0.93 V, that is, just after the first oxidation) so these oxidations are chemically irreversible. Multiple scans of this oxidative region (0.3 → 1.5 → 0.3 V) were also carried for **2** and **3** (Supporting Information, Figures S47 and S52). As for **1**, complex **2** exhibited sustained peak growth with each scan, and a similar colored material was deposited. In contrast, for complex **3**, the peak shape is destroyed and the current falls. This is consistent with the normal expectation that repeated cycles will deplete the concentration of nonoxidized compound at the surface, causing the current to drop. No deposition onto the electrode is observed for compound **3**. This is consistent with the lack of increased current, but is puzzling as a similar electropolymerization could have been expected. Interestingly, the butylene linked ligand and the copper(II) acetate complex of it have lower oxidation potentials than the ethylene and propylene analogues.

When scanning to negative potentials first (0 → −1.3 → 0 V) there is a single, low current irreversible reduction process observed for all complexes (**1**, E_{PC} −1.06 V; **2**, −1.07 V; **3**, −1.30 V), which results in an additional oxidation process or processes being observed on the return (**1**, E_{PA} −0.15 and 0.16 V; **2**, 0.18 V; **3**, 0.14 V; Supporting Information, Figures S32, S45 and S51). Scans to positive potentials first (0 → 1.5 → −1.3 → 0 V) result in additional reduction processes being observed (**1**, E_{PC} −0.06 and −0.43 V; **2**, 0.74 and 0.59 V; **3**, nil; Supporting Information, Figures S31 and S46). The reductive processes are likely to be the reduction either of the imines or of the copper centers ($Cu^{II} \rightarrow Cu^{I}$). Having acetate anions bound to the copper ions (as they will be in DCM) is expected to help make the reduction of these metal centers unfavorable, leading to quite negative E_{PC} values. The low current waves at about −1.1 V might well correspond to such a copper reduction, since imine reduction is expected to occur at even more negative potentials.[44] CVs following addition of a small amount of MeCN (1 mL) to the DCM solution were carried out to see if this copper(II) reduction could be shifted to more positive potentials. No shifting of any reductive process was observed. Presumably the acetate anions remain coordinated despite the presence of MeCN.

Copper(II) Tetrafluoroborate Macrocyclic Complexes. The electrochemistry of complexes **4**, **5**, and **6** was investigated in MeCN versus Ag/0.01 mol·L^{-1} $AgNO_3$ (Figure 9; Supporting Information, Figures S53−54, S58−59 and S63−65) as, unlike the DCM soluble and MeCN insoluble acetate analogues (**1**, **2**, and **3**), these tetrafluoroborate complexes are insoluble in DCM. The CVs of these complexes also exhibit distinct oxidation processes, having one large current oxidation wave and a number of smaller waves, sometimes seen as shoulders (**4**, E_{PA} 0.56 and 1.01 V; **5**, 0.61, 0.79, 0.95, and 1.45 V; **6**, 0.45, 0.55, 0.63, and 1.02 V). Once these values have been corrected for the differing cells, reference systems and solvent employed, by using the Fc/Fc^{+} couple as the internal reference in both cases, these E_{PA} values are all consistently higher than in the acetate complexes (**1**, **2**, and **3**). This is expected since there is a higher positive charge on the macrocyclic complex since the tetrafluoroborate is not bound, meaning the oxidation process occurs at a higher potential. These oxidation waves are almost entirely irreversible, as they were for the ligands. Only the ethylene complex, **4**, shows return reduction processes, wherein the first process has two accompanying, much smaller, peaks with E_{PC} of 0.45 and 0.22 V on the return scan. Multiple scans of this region (0/0.3 → 1.2/1.5 → 0/0.3 V) were also carried out for these tetrafluoroborate complexes, but no peak growth or deposition was observed (Supporting Information, Figures S57, S62 and S68). The oxidation product (as seen for the acetate analogues **1** and **2**) either is not being produced or it is being stabilized or solubilized by the MeCN solvent.

In scans to negative potentials first (0 → −2 → 0 V), these complexes also show several irreversible reduction processes (**4**, −0.19, −0.75, −1.15, and −1.30 V; **5**, −0.83 and −1.19 V; **6**, −0.57, −0.79, and −1.47 V). New oxidation waves are seen after scans to such potentials (**4**, 0 V {after scan to −2 V}; **5**, −0.45 and −0.05 V {after scan to lower than −1.19 V}; **6**, −0.41 {after scan to lower than −0.79 V}; Supporting Information, Figures S56, S61, and S66). Scans to positive potentials first (0 → 1.3 → −2 → 0 V) show markedly different reduction waves (Supporting Information, Figures S55, S60, and S67), likely a consequence of the irreversible oxidation events occurring prior to investigation of negative potentials. Reduction ($Cu^{II} \rightarrow Cu^{I}$) may be expected, and as neutral acetonitrile is bound, and is known for its ability to stabilize Cu^{I},[45] such a reduction would be significantly more favored than for the acetate complexes in DCM (implies E_{PC} expected to lie at higher potentials). Reduction of the copper(II) centers in the tetrafluoroborate complexes appears to happen in two steps, whereby one of the copper centers (E_{PC} ca. −0.8 V) seems to influence the other, causing a second reduction wave at slightly more negative potentials (E_{PC} ca. −1.2 V). If all of these reduction potentials are converted to be against the internal Fc/Fc^{+} couple (Table 2), for ease of comparison between the tetrafluoroborate complexes in MeCN versus Ag/0.01 mol·L^{-1} $AgNO_3$ and the acetate complexes in DCM versus Ag/AgCl (3 mol·L^{-1} KCl), these reductions are seen to occur at significantly more positive potentials, consistent with the tetrafluoroborate macrocyclic complexes carrying a higher charge than when acetate is bound. The remaining reduction processes in these complexes were not able to be explained.

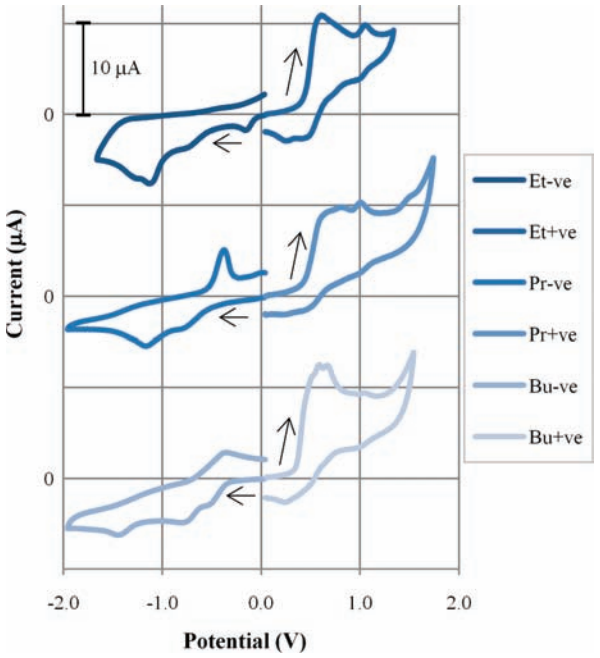

Figure 9. CVs of copper(II) tetrafluoroborate macrocyclic complexes **4**, **5**, and **6** run at 200 mV/s in MeCN versus Ag/0.01 mol·L^{-1} $AgNO_3$. Shown are two separate scans per complex, both starting from 0 V but one initially scanning to negative potentials and the other to positive potentials.

CONCLUSION

A simple high yielding metal-free synthesis of three Schiff base [2 + 2] macrocycles, the first to be obtained from the 2,2′-iminobisbenzaldehyde head unit, is presented. These macrocycles can be complexed with copper(II) acetate and tetrafluoroborate to give the corresponding, highly colored, macrocyclic complexes in good yields. The first structure determinations for any complex of a macrocycle derived from this head unit are reported. A square planar coordination environment is observed in the three complexes with coordinating acetate anions, whereas the use of the noncoordinating tetrafluoroborate anions led to a square pyramidal environment because of two molecules of solvent binding per copper(II) center. These new macrocycles provide two anionic N_3 terdentate binding pockets that we have proven in this study produce near 90° bond angles on binding

dx.doi.org/10.1021/ic200059n |*Inorg. Chem.* 2011, 50, 3697–3706

copper(II) ions. This is most encouraging as we look to extend this study to complexes of these macrocycles with other transition metal ions. These studies will also be greatly facilitated by the ease with which the pure metal-free macrocycles are isolated. This is a rare and advantageous situation, as most large Schiff-base macrocycles are only stable in the presence of a metal ion, necessitating considerably more synthetic effort to produce complexes of the range of transition metal ions of interest.

All of the compounds studied exhibited ligand based oxidations under 1 V. In the ethylene and propylene linked macrocyclic dicopper(II) acetate complexes in DCM these processes were quasi-reversible and generated a film on the electrode, consistent with an electropolymerization reaction having occurred. Practically nothing occurred in the reductive region of the CVs of the acetate complexes, owing to the solvent employed (DCM) and the bound anions. In contrast, the tetrafluoroborate complexes, studied in MeCN, exhibited multiple irreversible reductive steps, some of which are tentatively assigned to $Cu^{II} \rightarrow Cu^{I}$ reductions.

In summary, these results indicate that these new dinucleating Schiff base macrocycles have great promise: our next step is to explore other transition metal complexes of them.

EXPERIMENTAL SECTION

General Procedures. 2,2′-Iminobisbenzaldehyde and precursors were synthesized as described in the literature.[34] Diaminoalkanes and the copper(II) salts were of analytical reagent grade and used without further purification. Methanol for direct synthesis of the macrocycles was HPLC grade. IPA and pyridine (Py) were reagent grade.

General Method for Direct Synthesis of Imine [2 + 2] Macrocycles. To a refluxing solution of 2,2′-iminobisbenzaldehyde (~6 mmol, 1 equiv) in MeOH (120 mL) was added a standard solution in MeOH of the appropriate diaminoalkane (~6 mmol, 1 equiv). Within 20 min a bright yellow precipitate formed. The solution was refluxed for a further 2 h. Precipitate filtered, washed with ice-cold MeOH, and dried under vacuum (~80%).

Ethylene Linked Imine [2 + 2] Macrocycle (H_2L^{Et}). Using the general method above, reaction of the dialdehyde (1.4191 g, 6.300 mmol) with ethylene diamine (0.9991 M, 6.31 mL, 6.304 mmol) gave isolated pure product (1.3243 g, 84%). ESI(+) MS (m/z): 499.26 $[C_{32}H_{30}N_6H]^+$. Anal. Calcd for $C_{32}H_{30}N_6$: C, 77.08; H, 6.06; N, 16.85 Found: C, 77.19; H, 6.00; N, 16.67. ^{1}H NMR (300 MHz, $CDCl_3$) δ = 11.54 (NH, s, 2H), 8.49 (CHN, s, 4H), 7.58 (3-PhH, d [J = 7.5], 4H), 7.27 (6-PhH, d [J = 7.4], 4H), 7.21 (5-PhH, t [J = 7.6], 4H), 6.88 (4-PhH, t [J = 7.1], 4H), 3.96 (NCH_2, s, 8H). ^{13}C NMR (75 MHz, $CDCl_3$) δ = 163.14 (CHN), 143.44 (1-Ph), 131.30 (5-Ph), 131.07 (3-Ph), 123.38 (2-Ph), 120.36 (4-Ph), 117.51 (6-Ph), 62.22 (NCH_2). IR (KBr): (cm^{-1}) = 3010 (w), 2836 (w), 1630 (s), 1587 (s), 1534 (m), 1384 (m), 1456 (s), 1384 (m), 1316 (m), 1208 (w), 1150 (w), 1015 (w), 982 (w), 745 (s), 486 (w).

Propylene Linked Imine [2 + 2] Macrocycle (H_2L^{Pr}). Using the general method above, reaction of the dialdehyde (1.3231 g, 5.874 mmol) with propylene diamine (0.5006 M, 11.74 mL, 5.877 mmol) gave isolated pure product (1.2306 g, 80%). ESI(+) MS (m/z): 527.29 $[C_{34}H_{34}N_6H]^+$. Anal. Calcd for $C_{34}H_{34}N_6$: C, 77.54; H, 6.51; N, 15.96 Found: C, 77.30; H, 6.81; N, 16.08. ^{1}H NMR (300 MHz, $CDCl_3$) δ = 11.33 (NH, s, 2H), 8.52 (CHN, s, 4H), 7.59 (3 PhH, dd [J = 7.8, 1.8], 4H), 7.41 (6-PhH, dd [J = 8.4, 0.9], 4H), 7.27 (5-PhH, dt [J = 7.2, 1.8], 4H), 6.94 (4 PhH, dt [J = 7.5, 0.9], 4H), 3.73 (NCH_2, t [J = 7.2], 8H), 2.06 (NCH_2CH_2, quin [J = 7.2], 4H). ^{13}C NMR (75 MHz, $CDCl_3$) δ = 161.56 (CHN), 143.48 (1 Ph), 131.43 (3-Ph), 130.94 (5 Ph), 124.20 (2-Ph), 120.55 (4-Ph), 118.22 (6 Ph), 60.24 (NCH_2), 33.20 (NCH_2CH_2). IR (KBr): (cm^{-1}) = 2920 (w), 2818 (m), 1641 (s), 1577 (s), 1515 (s), 1451 (s), 1385 (m), 1310 (s), 1197 (w), 1156 (m), 1015 (w), 971 (w), 744 (s), 607 (w), 463 (w).

Butylene Linked Imine [2 + 2] Macrocycle (H_2L^{Bu}). Using the general method above, reaction of the dialdehyde (1.3845 g, 6.147 mmol) with butylene diamine (0.4415 M, 13.93 mL, 6.150 mmol) gave isolated pure product (1.2709 g, 75%). ESI(+) MS (m/z): 555.32 $[C_{36}H_{38}N_6H]^+$. Anal. Calcd for $C_{36}H_{38}N_6$: C, 77.95; H, 6.90; N, 15.15 Found: C, 78.07; H, 7.20; N, 15.34. ^{1}H NMR (400 MHz, $CDCl_3$) δ = 11.55 (NH, s, 2H), 8.53 (CHN, s, 4H), 7.64 (3 PhH, dd [J = 7.6, 1.2], 4H), 7.45 (6-PhH, d [J = 8.4], 4H), 7.28 (5-PhH, dt [J = 8.0, 1.6], 4H), 6.94 (4-PhH, t [J = 7.2], 4H), 3.65 (NCH_2, s, 8H), 1.80 (NCH_2CH_2, s, 8H). ^{13}C NMR (100 MHz, CDCl3) δ = 161.33 (CHN), 143.37 (1 Ph), 131.12 (3-Ph), 130.97 (5-Ph), 123.72 (2-Ph), 120.40 (4-Ph), 117.68 (6-Ph), 61.94 (NCH_2), 29.23 (NCH_2CH_2). IR (KBr): (cm^{-1}) = 3010 (w), 2939 (w), 2826 (m), 1628 (s), 1605 (w), 1587 (s), 1524 (s), 1454 (s), 1378 (m), 1312 (s), 1255 (w), 1199 (w), 1156 (w), 1125 (w), 1035 (w), 978 (w), 745 (s), 681 (m), 481 (w).

General Method A: Synthesis of Dicopper(II) Acetate Macrocyclic Complexes Derived from Imine [2 + 2] Macrocycles. To a refluxing light yellow suspension of the appropriate imine [2 + 2] macrocycle (1 equiv) in dry MeOH (20 mL, distilled over CaH_2) was added a light blue solution of $Cu(OAc)_2 \cdot H_2O$ (2 equiv) in dry MeOH (20 mL). The yellow suspension immediately changed to yellow-brown solution. Refluxed for further 3 h. Turned off heating, removed condenser, and left overnight, yielding X-ray quality crystals (dark orange-brown blocks) which were collected from the reaction vessel in good yields.

$[Cu^{II}_2L^{Et}(OAc)_2] \cdot H_2O$ (*1*). Using the general method A above, reaction of H_2L^{Et} (28.4 mg, 0.0570 mmol, 1 equiv) with $Cu(OAc)_2 \cdot H_2O$ (23.0 mg, 0.1152 mmol, 2.02 equiv) gave pure isolated product (37.6 mg, 73%). ESI(+) MS (m/z): 653.11 $[C_{32}H_{28}N_6Cu_2\ OMe]^+$, 560.17 $[C_{32}H_{28}N_6CuH]^+$. Anal. Calcd for $C_{36}H_{36}N_6Cu_2O_5$: C, 56.91; H, 4.78; N, 11.06 Found: C, 56.89; H, 4.62; N, 11.05. IR (KBr): (cm^{-1}) = 3427 (m, br), 3244 (w), 2916 (w), 1635 (s), 1612 (s), 1580 (s), 1552 (s), 1463 (m), 1432 (s), 1401 (s), 1314 (s), 1227 (m), 1190 (m), 1156 (m), 1036 (m), 749 (m), 676 (w), 462 (w). UV−vis: λ/nm (ε/L mol^{-1} cm^{-1}) = 249 (20,400), 280 (sh., 12,500), 335 (4,200), 405 (3,600), 486 (6,700), 910 (514).

$[Cu^{II}_2L^{Pr}(OAc)_2] \cdot MeOH \cdot 1.2H_2O$ (*2*). Using the general method A above, reaction of H_2L^{Pr} (25.7 mg, 0.0488 mmol, 1 equiv) with $Cu(OAc)_2 \cdot H_2O$ (19.9 mg, 0.0997 mmol, 2.04 equiv) gave pure isolated product (26.2 mg, 70%). ESI(+) MS (m/z): 709.14 $[C_{36}H_{35}N_6O_2\ Cu_2]^+$, 681.15 $[C_{34}H_{32}N_6Cu_2OMe]^+$. Anal. Calcd for $C_{39}H_{44.4}N_6Cu_2O_{6.2}$: C, 56.88; H, 5.43; N, 10.21 Found: C, 56.79; H, 5.24; N, 10.27. IR (KBr): (cm^{-1}) = 3419 (w, br), 2916 (w), 2854 (s), 1614 (s), 1552 (s), 1460 (m), 1435 (s), 1401 (m), 1323 (s), 1193 (m), 1162 (m), 1135 (m), 1020 (w), 749 (m), 670 (w), 474 (w). UV−vis: λ/nm (ε/L mol^{-1} cm^{-1}) = 251 (19,500), 275 (sh., 13,900), 333 (3,700), 396 (3,300), 471 (6,500), 880 (540).

$[Cu^{II}_2L^{Bu}(OAc)_2] \cdot 1.2H_2O$ (*3*). Using the general method A above, reaction of H_2L^{Bu} (40.5 mg, 0.0730 mmol, 1 equiv) with $Cu(OAc)_2 \cdot H_2O$ (30.5 mg, 0.153 mmol, 2.09 equiv) gave pure isolated product (28.5 mg, 44%). ESI(+) MS (m/z): 737.17 $[C_{38}H_{39}N_6O_2\ Cu_2]^+$, 709.14 $[C_{36}H_{36}N_6Cu_2OMe]^+$. Anal. Calcd for $C_{40}H_{44.4}N_6Cu_2O_{5.2}$: C, 58.62; H, 5.46; N, 10.25. Found: C, 58.55; H, 5.36; N, 10.19. IR (KBr): (cm^{-1}) = 3441 (w, br), 2914 (w), 2854(w), 1716 (w), 1618 (s), 1596 (s), 1554 (s), 1462 (m), 1435 (s), 1405 (s), 1318 (s), 1198 (m), 1153 (m), 1014 (w), 746 (m), 675 (w), 462 (w). UV−vis: λ/nm (ε/L mol^{-1} cm^{-1}) = 249 (20,200), 280 (sh., 11,100), 331 (4,000), 396 (3,300), 476 (7,300), 850 (542).

General Method B: Synthesis of Dicopper(II) Tetrafluoroborate Macrocyclic Complexes Derived from Imine [2 + 2] Macrocycles. To a hot (70 °C) light yellow suspension of the

appropriate imine [2 + 2] macrocycle (1 equiv) in IPA (30 mL) and Py (7 drops) was added a light blue suspension of $Cu(BF_4)_2 \cdot xH_2O$ (2 equiv) in IPA (15 mL). The yellow suspension slowly changed to a dark orange-brown solution over half an hour. Reduced the solvent volume to 10 mL, cooled, and then filtered and washed the resulting precipitate. The product was dried under vacuum.

$[Cu^{II}_2L^{Et}(Py)_2(OH_2)_2](BF_4)_2 \cdot 0.5H_2O$ (*4*). Using the general method B above, reaction of H_2L^{Et} (50.5 mg, 0.101 mmol) with $Cu(BF_4)_2 \cdot xH_2O$ (50.4 mg, 0.213 mmol) gave the desired orange-brown product (58.5 mg, 58%). ESI(+) MS (*m*/*z*): 560.172 $[CuL^{Et}H]^+$, 436.610 $[Cu_2L^{Et}(Py)_2F](H_2O)_4$, 341.082 $[Cu_2L^{Et}(IPA)]^{2+}$. Anal. Calcd for $C_{42}H_{43}N_8Cu_2B_2F_8O_{2.5}$: C, 50.42; H, 4.33; N, 11.20. Found: C, 50.52; H, 4.33; N, 10.85. IR (ATR):/cm^{-1} = 3538 (w, br), 3278 (w), 3054 (w), 2941 (w), 1611 (m), 1553 (m), 1527 (m), 1461 (m), 1433 (m), 1401 (w), 1307 (m), 1192 (m), 1157 (m), 1030 (s, br), 876 (w), 855 (w), 778 (m), 745 (s), 699 (w), 658 (w), 520 (m), 499 (m). UV−vis: λ/nm (ε/L mol^{-1} cm^{-1}) = 220 (33,800), 250 (33,000), 277 (sh., 13,300), 329 (3,610), 363 (4,390), 402 (4,780), 478 (6,830), 790 (413).

$[Cu^{II}_2L^{Pr}(Py)_2(OH_2)_{1.5}(IPA)_{0.5}](BF_4)_2$ (*5*). Using the general method B above, reaction of H_2L^{Pr} (53.9 mg, 0.102 mmol) with $Cu(BF_4)_2 \cdot xH_2O$ (50.5 mg, 0.213 mmol) gave the desired brown product (65.8 mg, 62%). ESI(+) MS (*m*/*z*): 588.202 $[CuL^{Pr}H]^+$, 465.636 $[Cu_2L^{Pr}(Py)_2(MeCN)_3]^{2+}$. Anal. Calcd for $C_{45.5}H_{49}N_8Cu_2B_2F_8O_2$: C, 52.50; H, 4.75; N, 10.77. Found: C, 52.50; H, 4.67; N, 10.65. IR (ATR): (cm^{-1}) = 3548 (w, br), 3268 (w), 2928 (w), 1609 (m), 1553 (m), 1536 (m), 1453 (m), 1434 (m), 1403 (w), 1313 (m), 1193 (m), 1157 (m), 1051 (s, br), 880 (w), 853 (w), 749 (s), 699 (w), 677 (w), 641 (w), 520 (m), 471 (m), 440 (w). UV−vis: λ/nm (ε/L mol^{-1} cm^{-1}) = 213 (19,800), 249 (21,700), 275 (sh., 10,300), 327 (3,710), 363 (3,730), 392 (4,430), shoulder at about 825 (ca. 800).

$[Cu^{II}_2L^{Bu}(Py)_2(OH_2)_2](BF_4)_2 \cdot$ IPA (*6*). Using the general method B above, reaction of H_2L^{Bu} (47.7 mg, 0.0860 mmol) with $Cu(BF_4)_2 \cdot xH_2O$ (42.3 mg, 0.1784 mmol) gave the desired golden-brown product (52.3 mg, 55%). ESI(+) MS (*m*/*z*): 616.24 $[CuL^{Bu}H]^+$, 546.17 $[Cu_2L^{Bu}(Py)_5F]^{2+}$. Anal. Calcd for $C_{49}H_{58}N_8Cu_2B_2F_8O_3$: C, 53.27; H, 5.02; N, 10.14. Found: C, 53.40; H, 4.78; N, 10.15. IR (ATR): (cm^{-1}) = 3548 (w, br), 2936 (w), 2865 (w), 1607 (m), 1554 (m), 1537 (m), 1463 (m), 1435 (m), 1409 (m), 1347 (w), 1313 (m), 1303 (m), 1261 (w), 1233 (w), 1197 (m), 1156 (s), 1134 (w), 1053 (s, br), 990 (m), 856 (w), 754 (s), 709 (w), 641 (w), 520 (w), 456 (m), 394 (m). UV−vis: λ/nm (ε/L mol^{-1} cm^{-1}) = 217 (28,700), 246 (23,100), 271 (17,100), 328 (3,800), 391 (3,800), 436 (5,200), 467 (7,200), 858 (450).

Instrumentation and Measurements. As reported previously,[46] except for the following.

See Supporting Information, Tables S1 and S2 for a summary of selected crystallographic data, data collection and structure refinement details.

All cyclic voltammetry (CV) experiments were carried out on solutions containing 1 mmol L^{-1} compound and 0.1 mol·L^{-1} $TBAPF_6$ electrolyte (Fluka >99%, used as received). Ligands and acetate complexes were run in DCM (filtered through a pad of neutral alumina) in a mini-cell (2 mL working volume), using a platinum (1 mm diameter) or glassy carbon (1.4 mm diameter) working electrode connected to a Ag/AgCl (3 mol·L^{-1} KCl) reference electrode (Cypress EE007 mini-Electrode) and a platinum wire serving as counter electrode. The tetrafluoroborate complexes were run in dry, distilled (over CaH_2) MeCN in a two-compartment three-electrode cell (5 mL working volume), using a platinum working electrode (1 mm diameter) connected to a Ag/0.01 mol·L^{-1} $AgNO_3$ reference electrode and a platinum plate serving as counter electrode. Measurements were recorded with an EG&G Princeton Applied Research Potentiostat/Galvanostat Model 273A unit at room temperature. The working electrode surface was cleaned using 0.015 μm alumina, washed with water and dried before every scan unless otherwise stated. The working volume was degassed by passing a stream of Ar through it for 15 min prior to the measurements and then maintaining an inert atmosphere of Ar over the solution during the measurements. E_m is the midpoint potential (approximately the reversible formal potential), calculated from the average of E_{PA} and E_{PC}. ΔE_P is the absolute value of the difference between E_{PA} and E_{PC}.

■ ASSOCIATED CONTENT

Supporting Information. Further details are provided in Figures S1−S68 and Tables S1−S7. This material is available free of charge via the Internet at http://pubs.acs.org. Supplementary crystallographic data can be obtained from the CCDC using the following reference codes: 796910 {2,2′-iminobis(ethyl benzoate)}, 796911 {2,2′-iminobisbenzaldehyde}, 796912 $\{H_2L^{Et}\}$, 796913 $\{H_2L^{Pr}\}$, 796914 $\{H_2L^{Bu}\}$, 796915 $\{[Cu^{II}_2(OAc)_2L^{Et}]\}$, 796916 $\{[Cu^{II}_2(OAc)_2L^{Pr}] \cdot 1.5MeOH \cdot 0.5H_2O\}$, 796917 $\{[Cu^{II}_2(OAc)_2\ L^{Bu}] \cdot 3MeOH\}$ and 796918 $\{[Cu^{II}_2(DMF)_4\ L^{Pr}](BF_4)_2 \cdot 2H_2O\}$. This data can be obtained free of charge from the Cambridge Crystallographic Data Centre via www.ccdc.cam.ac.uk/data_request/cif.

■ AUTHOR INFORMATION

Corresponding Author

*Fax: (+64)-3-4797906. E-mail: sbrooker@chemistry.otago.ac.nz.

■ ACKNOWLEDGMENT

We are grateful to the University of Otago for funding this research, including a Postgraduate Scholarship (to S.A.C.), and to Professor Alan Bond (Monash) for helpful discussions and suggestions regarding the electrochemistry results.

■ REFERENCES

(1) Pilkington, N. H.; Robson, R. *Aust. J. Chem.* **1970**, *23*, 2225–2236.
(2) Nelson, S. M. *Pure Appl. Chem.* **1980**, *52*, 2461–3476.
(3) Fenton, D. E. *Pure Appl. Chem.* **1986**, *58*, 1437–1444.
(4) Lindoy, L. F. *The Chemistry of Macrocyclic Ligand Complexes*; Cambridge University Press: Cambridge, U.K., 1990.
(5) Atkins, A. J.; Black, D.; Blake, A. J.; Marin-Becerra, A.; Parsons, S.; Ruiz-Ramirez, L.; Schroder, M. *Chem. Commun.* **1996**, 457–464.
(6) Okawa, H.; Furutachi, H.; Fenton, D. E. *Coord. Chem. Rev.* **1998**, *174*, 51–75.
(7) Reiter, W. A.; Gerges, A.; Lee, S.; Deffo, T.; Clifford, T.; Danby, A.; Bowman-James, K. *Coord. Chem. Rev.* **1998**, *174*, 343–359.
(8) Gerbeleu, N. V.; Arion, V. B.; Burgess, J. *Template Synthesis of Macrocyclic Compounds*. Wiley-VCH: Weinheim, Germany, 1999.
(9) Brooker, S. *Coord. Chem. Rev.* **2001**, *222*, 33–56.
(10) Brooker, S. *Eur. J. Inorg. Chem.* **2002**, 2535–2547 and front cover feature.
(11) Vigato, P. A.; Tamburini, S. *Coord. Chem. Rev.* **2004**, *248*, 1717–2128.
(12) Lozan, V.; Loose, C.; Kortus, J.; Kersting, B. *Coord. Chem. Rev.* **2009**, *253* (19−20), 2244.
(13) Love, J. B. *Chem. Commun.* **2009**, 3154–3165.
(14) Gagné, R. R.; Koval, C. A.; Smith, T. J. *J. Am. Chem. Soc.* **1977**, *99*, 8367–8368.
(15) Acholla, F. V.; Takusagawa, F.; Mertes, K. B. *J. Am. Chem. Soc.* **1985**, *107*, 6902–6908.
(16) Bailey, N. A.; Fenton, D. E.; Moody, R.; Rodriguez de Barbarin, C. O.; Sciambarella, I. N.; Latour, J.-M.; Limosin, D.; McKee, V. *J. Chem. Soc., Dalton Trans.* **1987**, 2519–2529.

(17) Brooker, S.; Hay, S. J.; Plieger, P. G. *Angew. Chem., Int. Ed.* **2000**, *39*, 1968–1970.
(18) Brooker, S.; Davidson, T. C.; Hay, S. J.; Kelly, R. J.; Kennepohl, D. K.; Plieger, P. G.; Moubaraki, B.; Murray, K. S.; Bill, E.; Bothe, E. *Coord. Chem. Rev.* **2001**, *216*−*217*, 3–30.
(19) Black, D.; Blake, A. J.; Finn, R. L.; Lindoy, L. F.; Nezhadali, A.; Rougnaghi, G.; Tasker, P. A.; Schroder, M. *Chem. Commun.* **2002**, 340–341.
(20) Depree, C. V.; Beckmann, U.; Heslop, K.; Brooker, S. *Dalton Trans.* **2003**, 3071–3081.
(21) Li, R.; Mulder, T. A.; Beckmann, U.; Boyd, P. D. W.; Brooker, S. *Inorg. Chim. Acta* **2004**, *357*, 3360–3368.
(22) de Geest, D. J.; Noble, A.; Moubaraki, B.; Murray, K. S.; Larsen, D. S.; Brooker, S. *Dalton Trans.* **2007**, 467–475.
(23) Jagoda, M.; Warzeska, S.; Pritzkow, H.; Wadepohl, H.; Imhof, P.; Smith, J. C.; Krämer, R. *J. Am. Chem. Soc.* **2005**, *127* (43), 15061–15070.
(24) Torelli, S.; Belle, C.; Gautier-Luneau, I.; Pierre, J. L.; Saint-Aman, E.; Latour, J. M.; Le Pape, L.; Luneau, D. *Inorg. Chem.* **2000**, *39* (16), 3526–3536.
(25) Tai, A. F.; Margerum, L. D.; Valentine, J. S. *J. Am. Chem. Soc.* **1986**, *108* (16), 5006–5008.
(26) Amendola, V.; Fabbrizzi, L.; Mangano, C.; Pallavicini, P.; Poggi, A.; Taglietti, A. *Coord. Chem. Rev.* **2001**, *219*−*221*, 821–837.
(27) Anbu, S.; Kandaswamy, M.; Suthakaran, P.; Murugan, V.; Varghese, B. *J. Inorg. Biochem.* **2009**, *103* (3), 401–410.
(28) Raman, N.; Sakthivel, A.; Rajasekaran, K. *J. Coord. Chem.* **2009**, *62* (10), 1661–1676.
(29) Sreedaran, S.; Shanmuga Bharathi, K.; Kalilur Rahiman, A.; Jagadish, L.; Kaviyarasan, V.; Narayanan, V. *Polyhedron* **2008**, *27* (13), 2931–2938.
(30) Collinson, S. R.; Fenton, D. E. *Coord. Chem. Rev.* **1996**, *148* 19–40.
(31) McKee, V. *Adv. Inorg. Chem.* **1993**, *40*, 323–399.
(32) Crichton, R. R. *Biological Inorganic Chemistry: An Introduction*; Elsevier: New York, 2008; p 369.
(33) Itoh, S. *Comprehensive Coordination Chemistry II* **2004**, *8*, 369–393.
(34) Black, D. S. C.; Rothnie, N. E. *Aust. J. Chem.* **1983**, *36* (12), 2387–2394.
(35) Borisova, N. E.; Reshetova, M. D.; Ustynyuk, Y. A. *Chem. Rev.* **2007**, *107* (1), 46–79.
(36) Menon, S. C.; Singh, H. B.; Patel, R. P.; Kulshreshtha, S. K. *J. Chem. Soc., Dalton Trans.* **1996**, *7*, 1203–1207.
(37) Panda, A.; Menon, S. C.; Singh, H. B.; Morley, C. P.; Bachman, R.; Cocker, T. M.; Butcher, R. J. *Eur. J. Inorg. Chem.* **2005**, *6*, 1114–1126.
(38) Lever, A. B. P. *Inorganic Electronic Spectroscopy*, 2nd ed.; Elsevier: New York, 1986; p 864.
(39) Hathaway, B. J. *J. Chem. Soc., Dalton Trans.* **1972**, 1196–1199.
(40) Addison, A. W.; Rao, T. N.; Reedijk, J.; van Rijn, J.; Vershoor, G. C. *J. Chem. Soc., Dalton Trans.* **1984**, 1349–1356.
(41) Patel, U.; Singh, H. B.; Butcher, R. J. *Eur. J. Inorg. Chem.* **2006**, *24*, 5089–5097.
(42) Menon, S. C.; Panda, A.; Singh, H. B.; Butcher, R. J. *Chem. Commun.* **2000**, *2*, 143–144.
(43) Waltman, R. J.; Bargon, J. *Can. J. Chem.* **1986**, *58* (20), 76–95.
(44) Andrieux, C. P.; Saveant, J. M. *J. Electroanal. Chem.* **1971**, *33* (2), 453–461.
(45) Kolthoff, I. M.; Coetzee, J. F. *J. Am. Chem. Soc.* **1957**, *79*, 1852–1858.
(46) Olguín, J.; Brooker, S. *New J. Chem.* **2011**, DOI: 10.1039/c0nj00774a.